

# Re-observing the EUV emission from Abell 2199: *in situ* measurement of background distribution by offset pointing

Richard Lieu<sup>1</sup>, Massimiliano Bonamente<sup>1</sup>, Jonathan P. D. Mittaz<sup>2</sup>, Florence Durret<sup>3</sup>, and Sergio Dos Santos<sup>3</sup> and Jelle S. Kaastra<sup>4</sup>

<sup>1</sup>Department of Physics, University of Alabama, Huntsville, AL 35899, U.S.A.

<sup>2</sup>Mullard Space Science Laboratory, UCL, Holmbury St. Mary, Dorking, Surrey, RH5 6NT, U.K.

<sup>3</sup>Institut d'Astrophysique de Paris, CNRS, 98bis Bd Arago, F-75014 Paris, France

<sup>4</sup>SRON Laboratory for Space Research, Sorbonnelaan 2, NL-3584 CA Utrecht, The Netherlands

Received \_\_\_\_\_; accepted \_\_\_\_\_

## ABSTRACT

The EUV excess emission from the clusters A2199 and A1795 remains an unexplained astrophysical phenomenon. There has been many unsuccessful attempts to ‘trivialize’ the findings. In this Letter we present direct evidence to prove that the most recent of such attempts, which attributes the detected signals to a background non-uniformity effect, is likewise excluded. We address the issue by a re-observation of A2199 which features a new filter orientation, usage of a more sensitive part of the detector and, crucially, includes a background pointing at  $\sim 2^\circ$  offset - the first *in situ* measurement of its kind. We first demonstrate quantitatively two facts: (a) the offset pointing provides an accurate background template for the cluster observation, while (b) data from other blank fields do not. We then performed point-to-point subtraction of the *in situ* background from the cluster field, with appropriate propagation of errors. The resulting cluster radial profile is consistent with that obtained by our original method of subtracting a flat asymptotic background. The emission now extends to a radius of 20 arcmin; it confirms the rising prominence of EUV excess beyond  $\sim 5$  arcmin as previously reported.

*Subject headings:* Galaxies: clusters: general; instrumentation: detectors; methods: data analysis, statistical; radiation mechanisms: thermal.

The origin of diffuse EUV and soft X-ray emission from the Virgo and Coma clusters of galaxies (Lieu et al 1996a,b), detected at a level higher than that expected from the hot intracluster medium (i.e. the cluster soft excess, or CSE, syndrome), has remained unsolved. The most serious theoretical puzzle is presented by the EUVE data of the rich clusters Abell 1795 and 2199, where the CSE emission was found to be very soft (with luminous EUV excess unaccompanied by any excess in the 1/4-keV band of the ROSAT PSPC) and

absent from the cluster centers (Mittaz, Lieu & Lockman 1998; Lieu, Bonamente & Mittaz 1999, hereafter abbreviated as LBM). The reported phenomena have profound implications irrespective of whether the emission turns out to be thermal, non-thermal, or some other origin (Cen & Ostriker 1999, Sarazin 1999, Lieu et al 1999 and references therein). It is therefore not surprising that questions concerning the observational integrity of CSE are still occasionally raised, especially with respect to A1795 and A2199. The area of data analysis being scrutinized recently is the subtraction of the EUVE detector background, as the inferred signals at large cluster radii, being only a small fraction of the background, are sensitive to this procedure.

To understand the potential problems involved in analysing data from the EUVE DS detector, we first describe the essential aspects of the DS background behavior which can affect the analysis of cluster data. We emphasize that here and after, unless otherwise specifically stated, only raw data (i.e. the output product of the EUVE standard telemetry processing pipeline, as publically archived) have been employed. The formidable problems which confront usage of additionally manipulated data will be enlisted shortly.

The portion of the DS occupied by the Lex/B (69 - 190 eV) filter is rectangular in shape, and the sensitivity of the detector to background photons and particles is not spatially uniform across this area<sup>1</sup>. In Figure 1 we show contours of the background as obtained by accumulating detector images of three extragalactic pointings, viz. 2EUVE J1100+34.4, 2EUVE J0908+32.6, and M15, totalling an exposure of  $\sim 85$  ksec, comparable to the longest exposure EUVE has in any single observation of an individual cluster. All bright sources have been removed. The figure results from a multi-scale wavelet analysis and reconstruction (see Slezak, Durret & Gerbal 1994) of the detector image, retaining

---

<sup>1</sup>Note that this sensitivity non-uniformity is *not* a vignetting effect, due to the obvious lack of azimuthal symmetry around boresight

features (in every spatial scale) which have a minimum significance level of  $3\sigma$ . It can be seen from Figure 1 that there is no evidence of extended emission at any scale, and that the background exhibits large scale gradients at the extremities of the y-axis. Note that this spatial pattern is typical of the DS Lex/B background for commensurate exposures. Thus, although such a 2-D view offers firm assurance that cluster glows are inherently not present in background fields, it also reveals the potential dangers of a 1-D view, viz. that any radial surface brightness profile centered at or near boresight (where clusters are usually observed) could lead to an underestimate of the background if this is taken from an annulus with large (inner and outer) radii which encompasses the bands of lower background.

Nonetheless, a simple way of minimizing this difficulty does exist, and (though not explicitly stated) has been the manner in which analysis leading to our past publications was performed. The same procedure is also adopted in the present work. It involves truncating areas of large and small y coordinate. There are no strict criteria on how to execute this, although our approach is to first plot the total detector counts as a function of y after they have been summed over all values of x, and then place the y-limits at the extreme ends of the ‘plateau’ region. To illustrate, we show in Figure 2 the y-profile of the composite detector image of many long exposure fields (Mrk 421, NGC 5548, PKS 2155-304, PSR J0108-1431, and the forementioned three fields, totalling an exposure of 0.736 Msec). It will be shown below, using the current data as example, that the method leads to a well-behaved background profile.

Other potential issues are the use of a template background and the effect of data manipulation. Detailed treatment of this subject is given in Kaastra (1999) but we summarize the main points here. A commonly used technique of ‘processing’ the raw data, known as *pulse height (PH) thresholding*, takes advantage of the fact that between the two main components of DS background, photon and particle, the former has a much narrower

range of PH. By selecting events within this range, it is possible in principle to suppress the particle background and improve the data signal-to-noise. In reality, however, the method only works for point sources. For diffuse emission, which illuminates a large area of the detector, the detector position dependence of this photon PH window complicates matters. Specifically, the entire window shifts towards higher PH as one moves from the central region of the detector where cluster centroids are usually located, to the outer regions where fainter radiation is detected from large cluster radii.

The common practice is to use a fixed PH window everywhere, even though this window corresponds only to the PH distribution of photon events at or near the detector center<sup>2</sup>. The result is a loss of photons, and consequently a decrease in the thresholded background, with increasing radius. This is the reason why Bowyer, Berghöffer, and Korpela 1999 (hereafter abbreviated as BBK) recently made the erroneous conclusion that cluster EUV, *including even the radiation of the hot gas*, are mere background effects. In fact, a map of the spatial distribution of the peak PH value of the photon PH window (Kaastra 1999) explains precisely why BBK find much steeper background gradients (relative to the raw data) across the DS detector. One could, of course, undertake the elaborate task of applying position dependent PH windows, as in the case of Kaastra (1999) who also subtracted a template background obtained from blank field pointings at random times and directions. Even after such efforts systematic uncertainties at a known level remain, because of the heavy data manipulations involved and the problems related to usage of a background template which is not obtained *in situ* (see below).

The decisive way of addressing these issues is to measure the true background

---

<sup>2</sup> A trivial way of PH thresholding the DS data, sometimes employed to remove detector artifacts, is to apply only a lower PH threshold. It introduces minimal bias to the data because off-axis photons, which are peaked at higher PH, are no longer excluded.

distribution of the detector region occupied by the cluster. We therefore scheduled an EUVE re-observation of A2199 in February 1999, which consisted of a 47 ksec exposure to the cluster (with the cluster center placed at 11.5 arcmin off-axis along the detector  $+x$  direction) immediately followed by a 11 ksec exposure of the blank sky region (on-axis J2000 coordinates of RA =  $245.523^\circ$ , DEC =  $40.326^\circ$ ,  $\sim 2^\circ$  offset from the cluster) whilst maintaining the same roll (azimuthal) angle of the Deep Survey (DS) detector. Within the context of the CSE this is the first direct approach to the EUVE deep survey (DS) detector background problem, as it involved a spatially and temporally contiguous observation - the data thus provided represents the most relevant background map for the purpose of subtraction.

The merits of using an offset pointing to estimate the cluster background are clear: the offset pointing background only differed from that of the cluster by 4% and this should be contrasted with the  $\sim 300$  % dynamic range of DS raw background values for the entire EUVE mission. Moreover, the two datasets were found to maintain their spatial distributions of event counts and pulse height (PH) over areas outside the cluster location, when again a broad variety of behavior exists within the archival database. To elaborate the latter point, we computed the difference between the radial profiles of the cluster and offset fields with the center of the annular system located at 15 arcmin from boresight along the detector  $-x$  direction. With this choice of center one avoids the effects of the cluster emission on the profile of the cluster field, since A2199 is  $\sim 27$  arcmin away on the other side of the detector. Thus one expects the subtraction to yield zero signal everywhere. This is indeed the case, as can be seen in Figure 3a, where the data follow a flat and vanishing profile with  $\chi^2_{red}(13) = 1.18$ , and the r.m.s. deviation is consistent with Poisson statistics - the residual point-to-point systematics are  $\sim 0.13$  % of the pre-subtracted flux. In contrast, when the procedure is repeated using the present cluster field but another offset background field acquired in the same month by pointing to a direction  $\sim 2^\circ$  away from the Virgo

cluster, the subtraction was not satisfactory, with  $\chi^2_{red}(13) = 4.41$ , and a large difference between the r.m.s. and Poisson errors indicating that even the residual point-to-point systematics are at a level higher than the random uncertainties. Thus, e.g., a region of apparent extended emission spanning  $\sim 6$  arcmin is evident in the innermost 10 arcmin of the subtracted profile, see Figure 3b. These comparisons clearly demonstrate the difficulties in building a background template from data obtained contemporaneously with the cluster observation: the only reliable template is that of a time contiguous, *in situ*, background.

In Figure 4a we show the radial profile of the offset background field, now with the annuli center placed at the detector position  $x = +11.5$  arcmin occupied by the centroid of A2199 during the cluster pointing. The data are consistent with a flat distribution out to  $\sim 28$  arcmin. Quantitatively, the difference between the 0 - 15 and 15 - 28 arcmin background levels is  $1.0 \pm 1.4\%$ .

As to the cluster field, we show in Figure 4b the sky radial profile of the raw data, taken from the same region of the DS detector as that of the background (offset) pointing. Comparison of Figure 4b with Figure 4a suggests that cluster emission extends to  $\sim 21$  arcmin, and one could proceed to obtain the cluster signals by subtracting a flat background as determined from the 21 - 28 arcmin region of the cluster field. In the present work, however, we undertake the most conservative approach by performing point-to-point subtraction of the offset background, with propagation of background errors. The cluster emission profile thus obtained is shown in Figure 5a, and the resulting soft excess profile in Figure 5b.

The rising importance of the CSE with radius, as reported in LBM (also Mittaz, Lieu, and Lockman 1998, on A1795), is confirmed by our re-observation of A2199. However, when compared with the original data (Figure 5b here versus Figure 1b of LBM) the CSE beyond 10 arcmin exhibits a steeper upward trend than previously. The reason has to do with the

new data revealing more emission in this region. The difference can be attributed to several features of the re-observation: (a) the availability of offset pointing enabled us to perform a more accurate background subtraction, (b) the exposure of the cluster to +11.5 arcmin off-axis location where the DS detector has relatively higher quantum efficiency because it has not been as exposed to bright sources as the normal locations near boresight (Kaastra 1999), and (c) the orientation of the DS detector, with the x-axis almost parallel to the celestial N-S direction, is at approximate right angles to that of the first observation - in this way the emission within 10 - 15 arcmin south-east of the cluster center, evident in the current data, was previously missed because it corresponded to large detector y-values, i.e. areas of lower sensitivity. To illustrate, we show in Figure 6 a combined image of the two observations (now totalling an exposure of 100 ksec), adaptively smoothed in the manner described in LBM. The emission in the extreme south east was not evident from the EUV contours of LBM.

The rising trend of the CSE suggests that its origin is a warm intracluster medium, with cooler gas residing at larger cluster radii, and large mass implications. Do the EUV signals represent the hitherto undetected baryons necessary to bridge the gap between theoretical and observational cosmology ? As an example we calculated the mass of the emitting gas between cluster radii of 12 and 15 arcmin, within the context of an equilibrium thermal model. The large EUV excess there, which is not accompanied by the detection of any soft X-ray excess in the 1/4-keV band of the ROSAT PSPC, constrains the gas temperature to  $kT \leq 10$  eV; the gas mass is then  $\sim 10^{14} M_{\odot}$ , on par with that of the dark matter in the same region of the cluster (Siddiqui, Stewart, & Johnstone 1998).

R. Lieu gratefully acknowledges support from NASA's ADP and EUVE-GI programs.

## References

Bowyer, S., Berghöffer, T., & Korpela, E., 1999, *Proc. of workshop on 'Thermal and*

*Relativistic Plasmas in Clusters of Galaxies*', Schlöss Ringberg, Germany, ed. H. Böhringer (also *astro-ph* 9907127).

Cen, R., & Ostriker, J.P. 1999, *ApJ*, **514**, L1.

Kaastra, J.S., Lieu, R., & Mittaz, J.P.D., 1999, *A & A*, in preparation.

Lieu, R., Mittaz, J.P.D., Bowyer, S., Lockman, F.J., Hwang, C. -Y., Schmitt, J.H.M.M. 1996a, *Astrophys. J.*, **458**, L5–7.

Lieu, R., Mittaz, J.P.D., Bowyer, S., Breen, J.O., Lockman, F.J., Murphy, E.M. & Hwang, C. -Y. 1996b, *Science*, **274**, 1335–1338.

Lieu, R., Ip W.-I., Axford, W.I. and Bonamente, M. 1999, *ApJL*, **510**, 25–28.

Lieu, R., Bonamente, M., & Mittaz, J.P.D. 1999, *ApJ*, **517**, L91.

Mittaz, J.P.D., Lieu, R., Lockman, F.J. 1998, *Astrophys. J.*, **498**, L17–20.

Morrison, R. and McCammon D., 1983, *ApJ*, **270**, 119–122.

Sarazin, C.L. 1999, *ApJ*, 520, 529.

Siddiqui, H., Stewart, G.C., & Johnstone, R.M., 1998, *A & A*, 334, 71.

Slezak, E., Durret, F., & Gerbal, D. 1994, *AJ*, **108**, 1996.

## Figure Captions

Figure 1. Greyscale map of the surface brightness of the DS as obtained by co-adding the detector image of three separate pointings (details see text) totalling an exposure of  $\sim 85$  ksec. The contours are scaled linearly between the maximum and minimum brightness values, which differ by 13 %. The normal convention adopted for the detector axes is also indicated, with tickmarks in units of detector pixels (13 pixels  $\sim 1$  arcmin) and with the on-axis (boresight) position at pixel coordinates (1024,1024).

Figure 2. The total intensity distribution of the DS along the detector y-axis. The dashed

line represents a strip where bright point sources affected the background - this region is therefore not shown. The dotted lines mark those y-limits beyond which the profile steepens considerably. In computing radial profiles only the y pixels within these limits were used. The data were obtained by merging many detector images (see text).

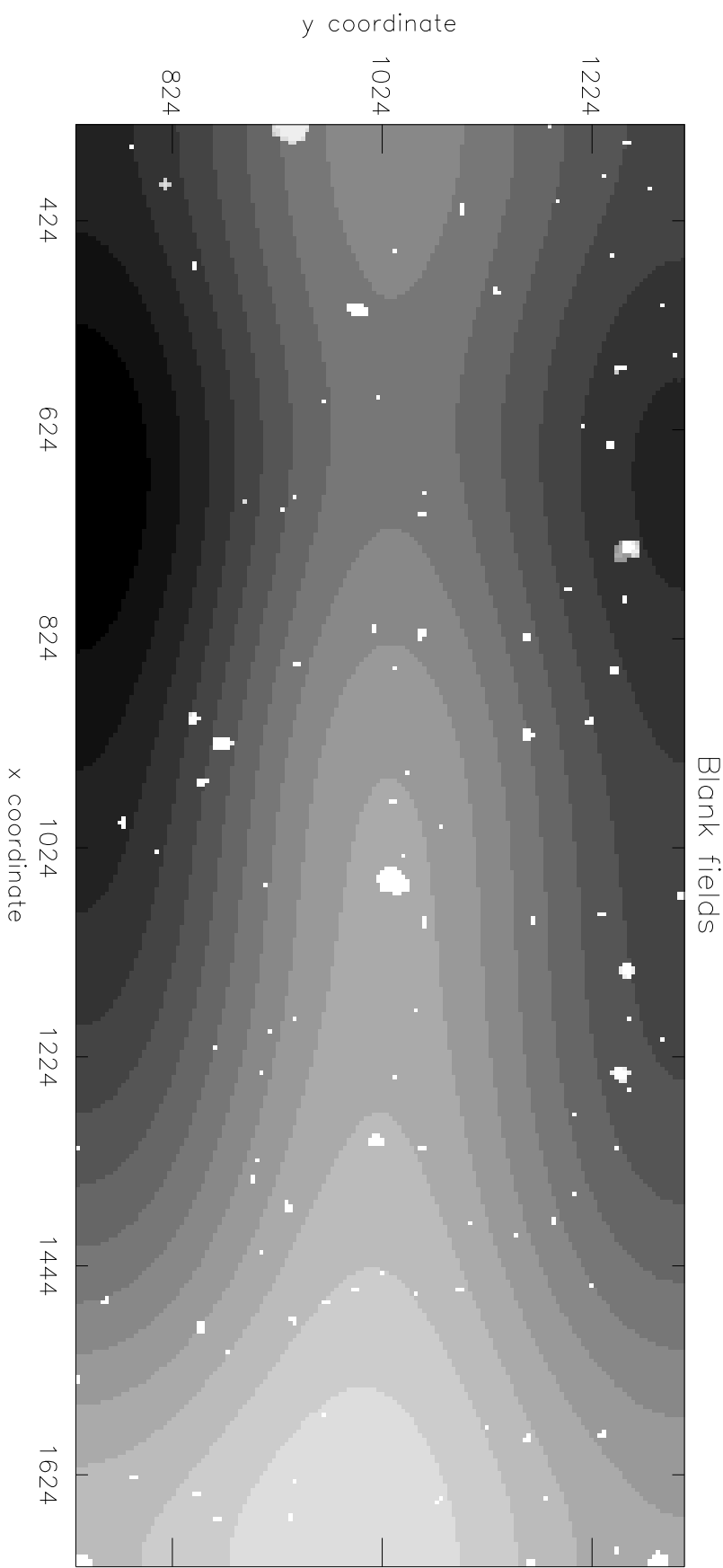
Figure 3. Radial profile of the A2199 cluster field, after subtracting the same profile of a background field. Both profiles are centered at an identical highly off-axis detector position far away from the detector region employed to observe A2199 (see text). 3a: the background field is that of the A2199 offset pointing; to eliminate the slight ( $\sim 4\%$ ) difference between the background of the cluster and offset pointing, the subtraction was performed after the offset profile was re-normalized such that the average asymptotic (21 - 28 arcmin) background agrees between the two fields - a procedure adopted to extract the actual cluster signals (Figure 5). 3b: the background field is that of a very different sky direction (see text), with the same re-normalization having been applied. Both plots are binned in 3 arcmins to reveal the presence or otherwise of large scale features produced by the subtraction. The data used are raw (i.e. no PH thresholding) and areas of known detector artifacts were excluded from analysis. This statement also applies to Figures 4 and 5.

Figure 4. Radial profiles of the offset (4a) and cluster (4b) pointings of the A2199 observation. The radius is measured from the detector position occupied by the emission centroid of A2199 in the cluster field. Dotted line represents the average brightness of the 21 - 28 arcmin region. For perusal of the cluster emission the data here are plotted in higher resolution than that of Figure 3, with the offset profile displayed in 2 arcmin bins to reduce the larger random uncertainties which result from the smaller exposure.

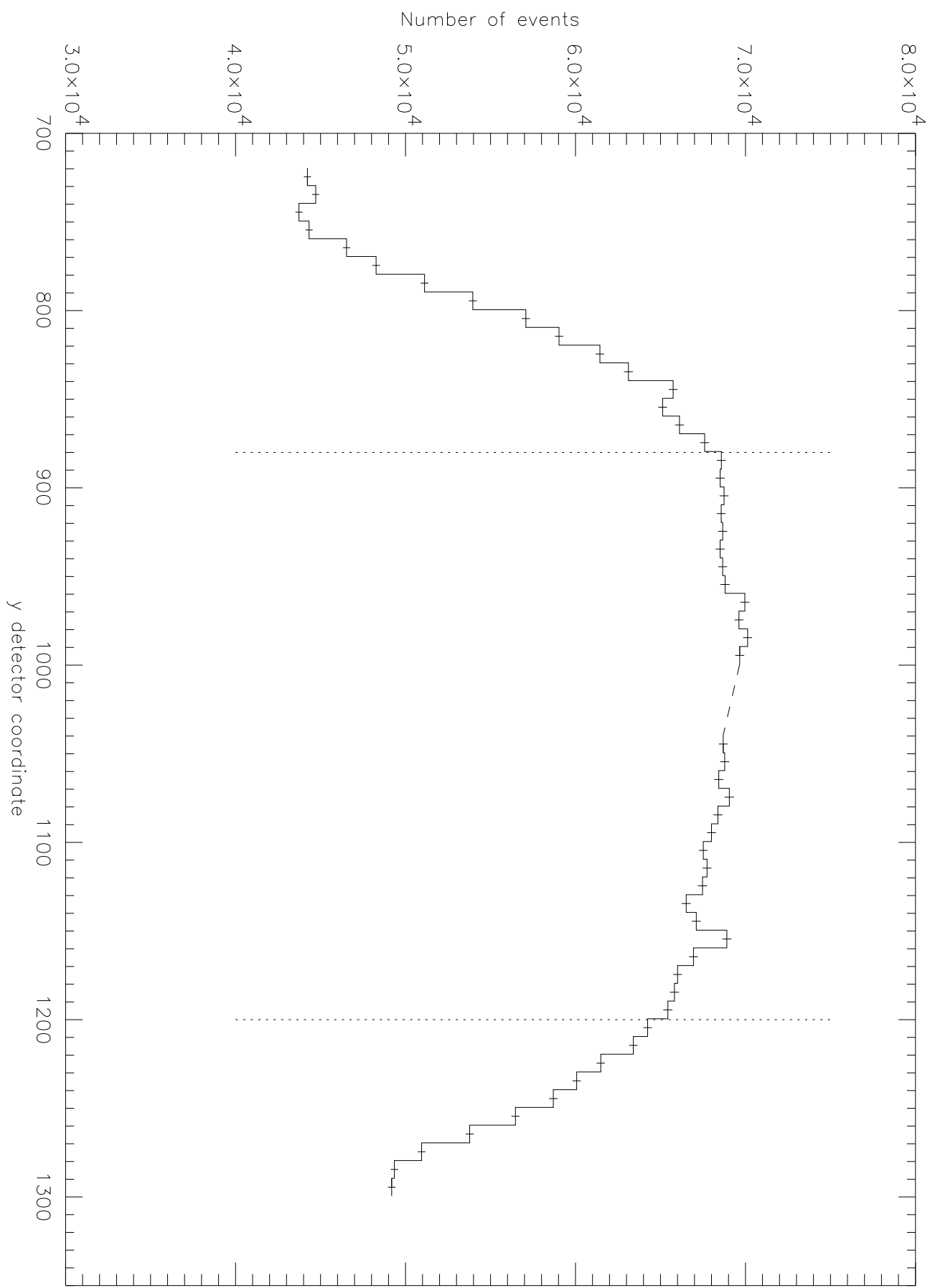
Figure 5. Radial profile of the A2199 cluster EUV signal (5a) and soft excess (5b), obtained by point-to-point subtraction of the background (offset) profile, with propagation of errors

from the background data and after scaling away the  $\sim 4\%$  difference between the 21 - 28 arcmin average background levels of the source and offset pointings. In 5b the C-band fluxes correspond to PSPC channels 18 - 41, and the expected Lex/B to C-band ratio of the hot ICM emission as given by the dashed line was computed in the manner of LBM (Figure 1b, except that the corresponding line there was lower because the interstellar absorption code adopted here (Morrison & McCammon 1983) involves removal of less extragalactic EUV signals than before). The lower fluxes in the inner radii may be due to intrinsic absorption.

Figure 6. Adaptively smoothed image of the two EUVE observations of A2199. Contours are cluster EUV emission brightness in units of photons  $\text{arcmin}^{-2} \text{ s}^{-1}$ .

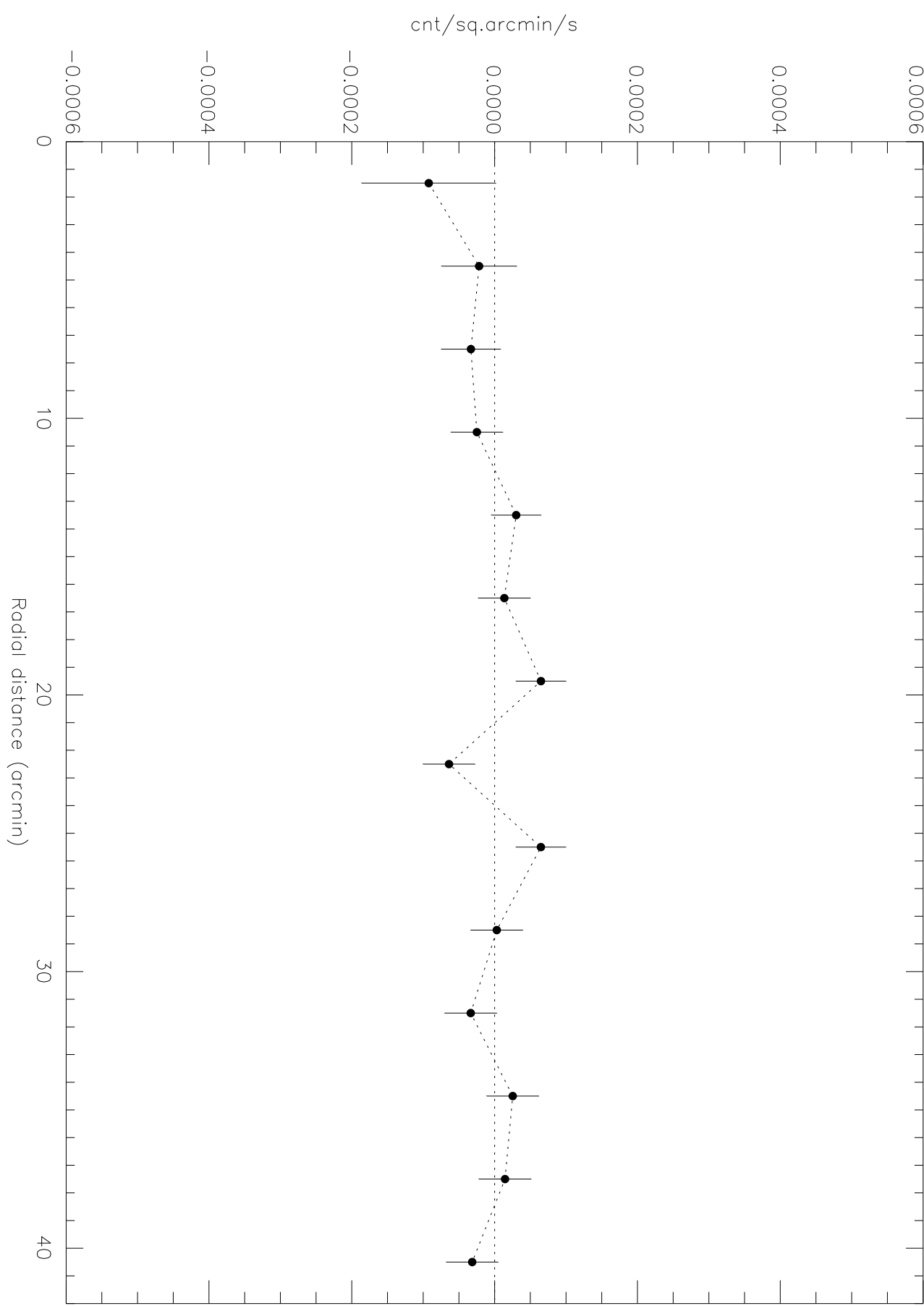






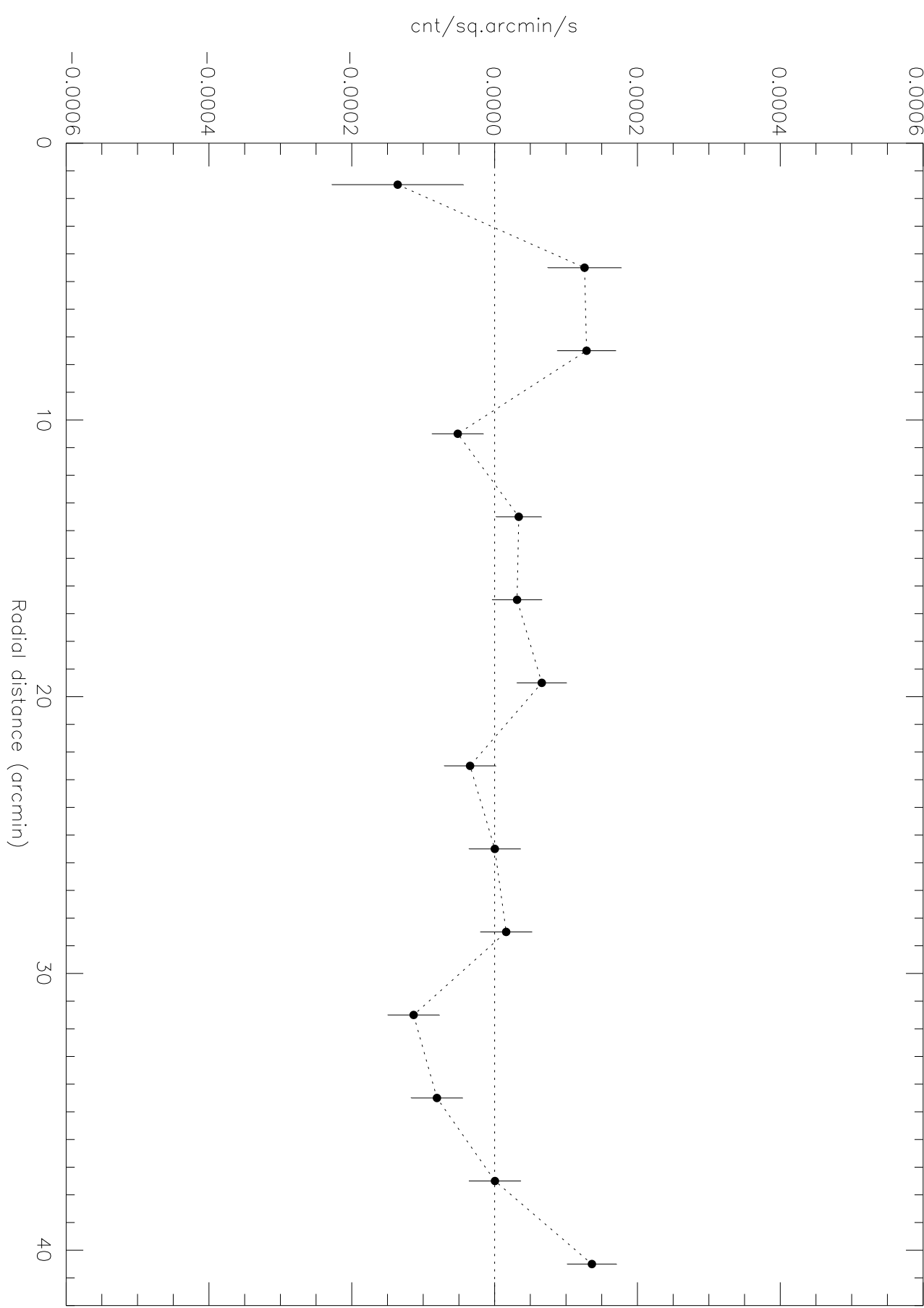


A2199 – A2199 off-set

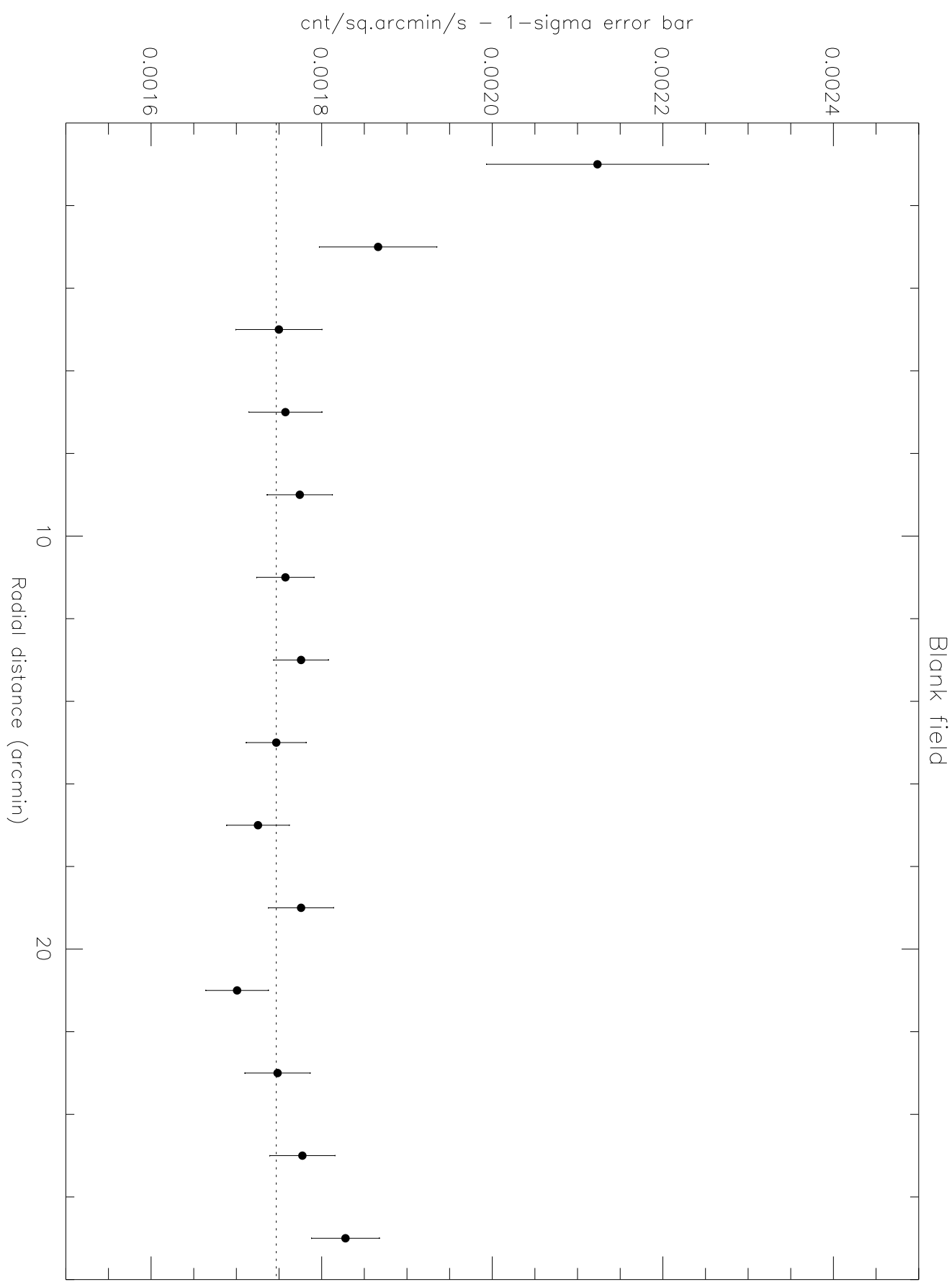




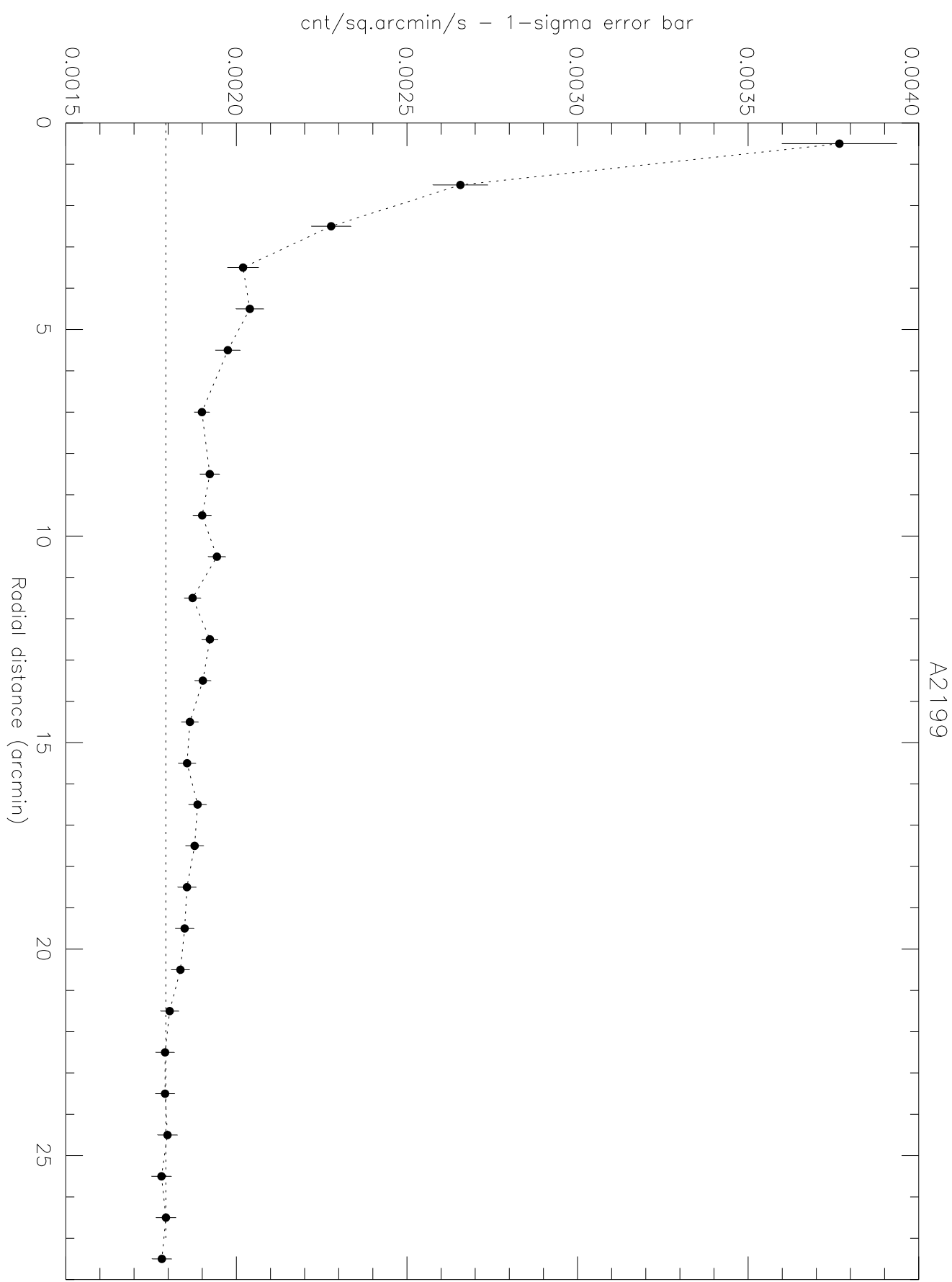
A2199 – Virgo off-set





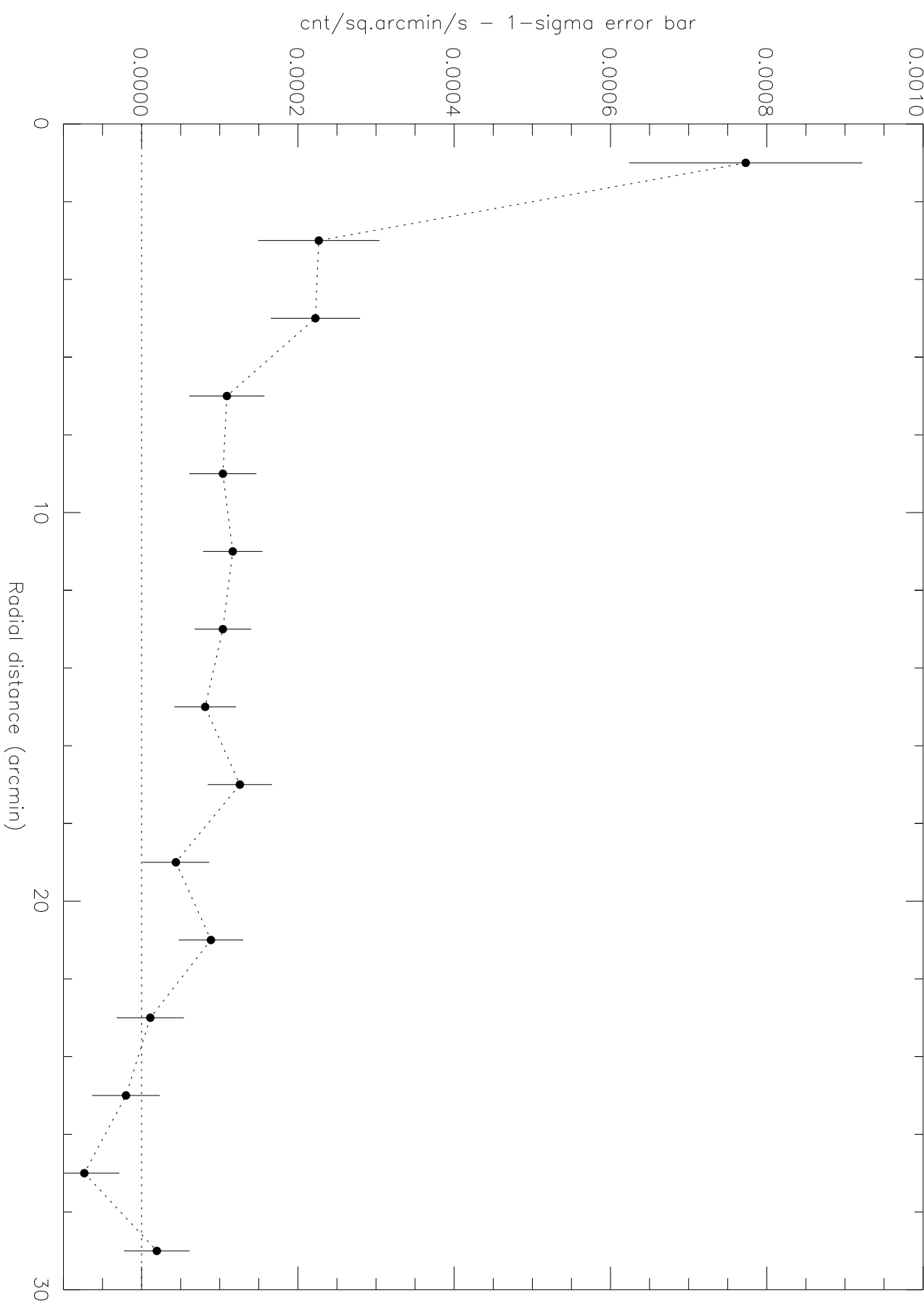








A2199 – off-set background subtracted





Lexan/B-to-PSPC/Carbon band count ratio

